

Modulation Order and Code Rate Optimisation for Digital Coherent Transceivers using Generalised Mutual Information

Robert Maher, Alex Alvarado, Domaniç Lavery and Polina Bayvel

Optical Networks Group, Department of Electronic & Electrical Engineering, University College London, Torrington Place, London WC1E 7JE, United Kingdom, r.maher@ucl.ac.uk

Abstract We experimentally demonstrate that generalised mutual information can be used as a design rule to select the optimal modulation order and code rate for SNR limited DP-mQAM transceivers. FEC overheads between 9% and 194% are shown to maximise spectral efficiency.

Introduction

The combination of advanced multi-level modulation formats, spectral shaping and forward error correction (FEC), is an essential requirement for optical communications systems to achieve high spectral efficiency (SE) and high sensitivity. Coded modulation (CM) in optical communications has typically employed hard decision (HD) FEC as it offers a good trade-off between performance and complexity. However, to further increase the SE, current state-of-the-art transceivers use a combination of soft decision (SD) FEC and higher-order modulation formats.

For SD-FEC decoders, the maximum SE (assuming ideal Nyquist filtering) is given by the mutual information (MI) between the transmitted and received symbols. MI has been recently proposed as a figure of merit for the characterisation of optical systems that utilise SD-FEC and has been verified through numerical simulations¹⁻³. The use of MI to predict the post-FEC bit error ratio (BER) of a SD-FEC implementation was also demonstrated experimentally for an optical system based on the dual polarisation (DP) differentially encoded quadrature phase shift keyed (QPSK) format⁴. Recently, we have experimentally demonstrated the use of MI to determine the maximum SE in 64 quadrature amplitude modulation (QAM) and 256QAM wavelength division multiplexed (WDM) transmission systems^{5,6}.

Bit-interleaved coded modulation (BICM)⁷ has proved an attractive design paradigm for CM with SD-FEC, as it decouples the detection process into two steps: de-mapping followed by SD binary decoding. This (sub-optimal) receiver structure operates on bits rather than symbols; therefore the MI does not define the maximum SE for this popular CM architecture⁸. Conversely, a related metric known as the generalised MI (GMI), does define the maximum SE for a BICM-based transceiver and thus, provides an accurate pre-

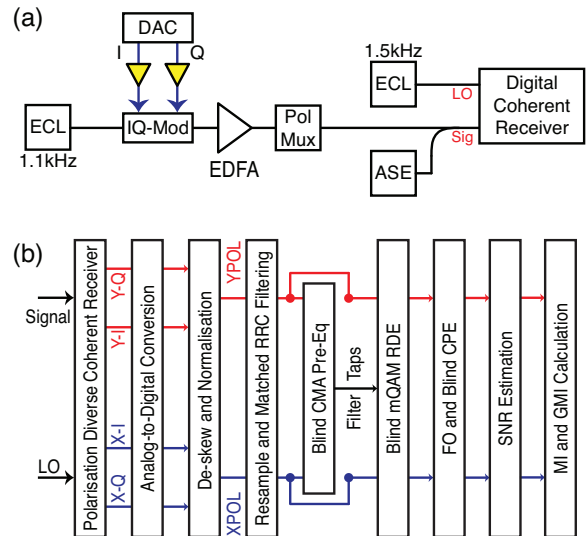


Fig. 1: (a) Single channel Nyquist shaped 8GBd DP-mQAM experimental setup and (b) DSP functions

diction of the performance of capacity approaching SD-FEC⁸.

In this work, we experimentally demonstrate for the first time, that the GMI can be used to select the optimum modulation order and code rate (defined as the number of input bits per output bit from the FEC decoder) in a Nyquist shaped DP-mQAM optical system. This back-to-back characterisation is sufficient to provide the maximum SE for a given BICM-based transceiver and thus, defines an upper limit on the achievable performance for the corresponding transmission system.

Experimental Setup

The experimental setup used in this work is illustrated in Fig. 1(a). The multi-level drive signals required for mQAM, where $m \in \{4, 16, 64, 256\}$, were generated offline and digitally filtered using a root raised cosine (RRC) filter with a roll-off factor of 0.01. The resulting in-phase (I) and quadrature (Q) signals were output using two digital-to-analogue converters (DACs) operating at 32GSa/s (4Sa/sym) and were subse-

quently amplified using two linear amplifiers before being applied to an IQ modulator. The output of an external cavity laser (ECL) with a 1.1kHz linewidth was passed directly into the modulator before being optically amplified and polarisation multiplexed to form an 8GBd Nyquist shaped DP-mQAM optical carrier. The DP-mQAM signal was passed into the signal port of the digital coherent receiver, which had a sample rate of 160GSa/s and an electrical analog bandwidth of 63GHz. Amplified spontaneous emission (ASE) noise was added to the signal to vary the received signal-to-noise ratio (SNR) and a second ECL (1.5kHz linewidth) was used as a local oscillator (LO).

The key blocks of the blind digital signal processing (DSP) implementation are illustrated in Fig. 1(b). The single-carrier DP-mQAM signal was initially compensated for receiver skew and the different responsivities of the balanced photodiodes. Each polarisation was resampled to 2Sa/sym before matched RRC filtering. A blind 51-tap radially directed equaliser (RDE) was used to equalise the signal and to undo polarisation rotations, with the constant modulus algorithm (CMA) equaliser used for pre-convergence. The frequency offset (FO) was subsequently removed prior to blind carrier phase estimation (CPE). The SNR of the optical signal was ideally estimated as the ratio between the variance of the transmitted symbols ($\mathbb{E}[|X|^2]$) and the variance of the noise (N_0), where $N_0 = \mathbb{E}[|Y - X|^2]$ and Y represents the received symbols. Finally, the MI and GMI were calculated from the received data using Monte Carlo integration.

MI and GMI Analysis

The MI was calculated over both polarisations as a function of the estimated SNR for 4, 16, 64 and 256QAM respectively and is shown in Fig. 2(a). The experimental measurement was recorded by adding ASE noise to the signal and measuring the MI for 50 discrete values of SNR ranging from 0dB to 24dB. The Shannon capacity, as defined by, $C = 2\log_2(1 + \text{SNR})$, is also displayed to provide a performance reference for our system. For DP-4QAM, the MI was 1.95b/sym at a SNR of 0dB and increased to 4b/sym as the SNR approached 11dB. Similar performance was achieved for DP-16QAM and DP-64QAM, with an approximately equal MI at a SNR of 0dB, with both formats reaching their maximum MI of 8b/sym and 12b/sym at received SNRs of 17.5dB and 24dB respectively.

The DP-256QAM format achieved a MI rang-

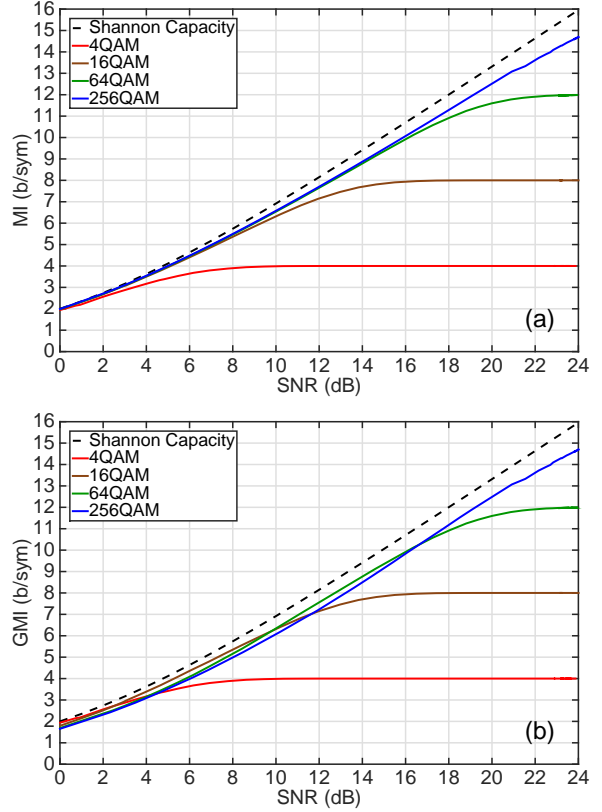


Fig. 2: (a) Experimentally measured MI as a function of the received SNR for each dual polarisation mQAM format and (b) corresponding GMI for each format

ing from 1.95b/sym at the lowest recorded SNR to a maximum of 14.72b/sym at a received SNR of 24dB. This value of MI is below the maximum of 16b/sym and illustrates the importance of estimating the in-band SNR as apposed to the more conventional optical SNR (OSNR). As the OSNR was increased to over 40dB, the in-band SNR, as measured in our DSP implementation, saturated at ~ 24 dB. This saturation in SNR occurred for all formats and was fundamentally transceiver limited, as explained below.

The key subsystems that limited the SNR were the DAC and linear electrical amplifier in the transmitter and the receiver electronics within the digital sampling oscilloscope. If higher order QAM formats, such as 1024QAM or 4096QAM, were generated with this transceiver setup, the ultimate performance in terms of bits per symbol would be approximately equal to 256QAM, due to this practical SNR limit. It is important to note that the MI curves for all formats never intersect, therefore it is always more spectrally efficient to choose the largest constellation size for any received SNR.

As mentioned previously, MI does not define the achievable SE for BICM-based optical systems, therefore we must consider the GMI. The

corresponding GMI as a function of received SNR for all formats is shown in Fig. 2(b). It is clear from this characterisation that the GMI curves intersect and that there are distinct SNR regimes where one modulation format exhibits a higher SE. There is also a slight penalty relative to the MI due to the sub-optimality of bit-wise decoders.

In the low SNR regime ($<2.5\text{dB}$) it is more efficient to use the DP-4QAM format, however DP-16QAM becomes more spectrally efficient for values of SNR between 2.5dB and 9.8dB . As expected, the greatest performance is again achieved using DP-256QAM, with a maximum GMI of 14.71b/sym , recorded at a saturated SNR of 24dB . The GMI provides the optimum modulation order as a function of SNR, but does not directly indicate what the minimum required code rate is in order to realise the achievable SE.

Normalised GMI

The normalised GMI is obtained by dividing the recorded GMI for each format by $2\log_2(M)$ and provides the minimum required code rate to achieve the maximum number of bits per symbol that can be reliably transmitted through the channel for a given SNR. Fig. 3 shows the normalised GMI as a function of the received SNR for all four formats. The dashed lines illustrate the optimum SNR when the constellation size should be increased in order to achieve the greatest SE.

For example, at a SNR above 2.5dB , it is more spectrally efficient to use the DP-16QAM format with a code rate of 0.34 (corresponding to a FEC overhead (OH) of 194.12%) than the DP-4QAM format with rate 0.679 (FEC OH: 47.27%). This is a key observation and demonstrates that depending on the SNR performance of a given system, the net bit rate can be maximised by considering very high FEC OHs, which far exceed that of currently installed optical communications systems. Not only is the optimum switching point observed with this experimental characterisation, but the required code rate within the SNR range of each modulation format is also recorded. The optimal modulation format switches to DP-64QAM at a SNR of 9.8dB and a code rate of 0.52 (FEC OH: 92.31%). Finally, the DP-256QAM format provides the greatest SE at any SNR above 16.63dB .

This experimental characterisation represents the maximum achievable performance for each of these binary reflected Gray coded DP-mQAM constellations. However, the gap between the recorded GMI and the Shannon capacity, as shown in Fig. 2(b), can be reduced for each mod-

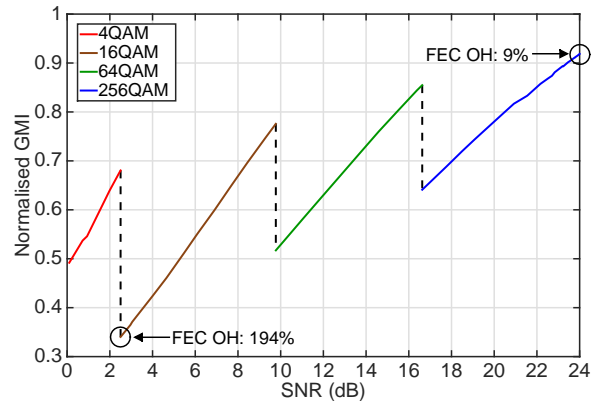


Fig. 3: Experimentally measured normalised GMI as a function of SNR. The dotted lines indicate the optimum SNR to increase the cardinality of the modulation format

ulation format if the constellations are probabilistically shaped at the transmitter⁹. This would provide a higher GMI for each format in the low SNR regime, although the maximum GMI would still ultimately be bounded by $2\log_2(M)$ bits per symbol.

Conclusions

We have experimentally demonstrated, for the first time, that the GMI performance metric can fully characterise the optimal modulation order and code rate of a SNR limited BICM-based transceiver. The maximum SE is achieved by tailoring the constellation size and the FEC OH based on the SNR achieved after digital coherent detection. The normalised GMI characterisation provides an excellent methodology to determine the performance limit of a digital coherent transceiver.

Acknowledgements

The support under the UK EPSRC Programme Grant UNLOC (UNLocking the capacity of Optical Communications) EP/J017582/1 is gratefully acknowledged.

References

- [1] R.-J. Essiambre et al., "Capacity Limits of Optical Fiber Networks," *J. Lightwave Technol.*, Vol. **28**, pp. 662 (2010).
- [2] I.B. Djordjevic et al., "Achievable Information Rates for High-Speed Long-Haul Optical Transmission," *J. Lightwave Technol.*, Vol. **23**, pp. 3755 (2005).
- [3] T. Fehenberger et al., "On Achievable Rates for Long-Haul Fiber-Optic Communications," *Opt. Express*, Vol. **23**, pp. 9183 (2015).
- [4] A. Leven et al., "Estimation of Soft FEC Performance in Optical Transmission Experiments," *IEEE Photon. Technol. Lett.*, Vol. **23**, pp. 1547 (2011).
- [5] D.S. Millar et al., "Transceiver-Limited High Spectral Efficiency Nyquist-WDM Systems," *Proc. OFC*, Th2A.13 (2015).
- [6] R. Maher et al., "Reach Enhancement of 100% for a DP-64QAM Super-Channel using MC-DBP," *Proc. OFC*, Th4D.5 (2015).
- [7] L. Szczecinski and A. Alvarado, "Bit-Interleaved Coded Modulation: Fundamentals, Analysis and Design," Wiley & Sons, ISBN: 978-0-470-68617-1 (2015).
- [8] A. Alvarado and E. Agrell, "Four-Dimensional Coded Modulation with Bit-Wise Decoders for Future Optical Communications," *J. Lightwave Technol.*, Vol. **33**, pp. 1993 (2015).
- [9] T. Fehenberger et al., "LDPC Coded Modulation with Probabilistic Shaping for Optical Fiber Systems," *Proc. OFC*, Th2A.23 (2015).